

# Optimal Design of a Permanent Magnet Synchronous Motor for High Efficiency and Low Cogging Torque

Ali Izanlo, S. Asghar Gholamian, and S. Ehsan Abdollahi

Babol Noshirvani University of Technology, Babol, Iran  
izanlo\_ali@yahoo.com

*Abstract:* In this paper, a new method is proposed for design and optimization of a Permanent Magnet Synchronous Motor (PMSM). In this method, the Particle Swarm Optimization (PSO) algorithm is combined with Finite Element Analysis (FEA) and information is exchanged between them online. This information is cost functions and optimization variables. Four parameters that are related to magnets and slots of machine i.e. pole offset, magnet thickness, pole embrace, and stator slot dimension are used as optimization variables in the PSO algorithm, also efficiency and cogging torque are selected as cost functions. In each iteration, optimization variables enter to the PSO algorithm from FEA, then cost function is calculated and results are sent back to the FEA. This process is iterated until the best variables is gained to maximize or minimize the cost function. Also at the beginning, a parametric study is performed on the geometrical dimension of permanent magnets and stator slots to analyze the effects of dimensions variations on efficiency and cogging torque. Permanent magnets and stator slots dimensions are then optimized using PSO algorithm for optimal performance of PMSM. Results of design and optimization show effectiveness and capability of proposed method.

*Keywords:* Design process, PMSM, Cogging Torque, Optimization, PSO Algorithm

## 1. Introduction

PMSMs has several advantages such as high torque density, high efficiency and high power factor, but an important drawback of this machine is cogging torque which causes noise and shaft vibration. Moreover cogging torque causes in pulsating in motor and prevents having a smooth rotation, specially at light loads and low speed [1-4].

PMSM design for variable applications done in multiple literature and paper [5-9]. In [5], a PMSM designed for electric vehicles in automotive industry. In order to achieve high dynamic performance and high efficiency a multi-objective optimization design method based on the artificial bee colony algorithm proposed. In [6], a five-phase permanent magnet synchronous machine was investigated. It has features such as high power density and high fault tolerant capability for electric vehicles. In [7], comprehensive design of a low speed 4 kW, 240 Nm and 159.2 min<sup>-1</sup> PMSM for gearless elevators evaluated and simulated by using FEA and the results are validated with the analytical calculations. A new method for achieving maximum efficiency and power density of PMSM was provided in [8] using the bees algorithm for industrial applications. In [9], design and optimization of a PMSM for use in hydrodynamic renewable energy is proposed. At first, analytical calculations and the design process of PMSM explained. Then, ant colony optimization algorithm used for the optimization of design quantities.

There are different method for increase of efficiency and cogging torque reduction [10-15]. According to different applications and considerations of technical and economical factors, various cogging torque reduction methods can be employed, such as slot or magnet skewing, magnet pole shape optimization and stator slot opening width optimization etc [10]. Optimal dimension of magnet embrace affects the cogging torque and efficiency [11]. A classical one is choosing magnet pole span, an integer multiple of slot pitch, this solution reduces the magnitude of the first order harmonic of cogging torque [12]. Another recommended technique is teeth pairing with different tooth width [13]. In [14], a stator structure with auxiliary teeth proposed and studied for reducing cogging torque in outer rotor PMSM. In [15], in order to solve this

problem, the cogging torque calculated as a function of skewing angle of the magnets and by an appropriate skewing, the cogging torque can be reduced to half theoretically.

In this paper, a new method is proposed for optimization of PMSM. Optimization goals are reduce of cogging torque and increase of efficiency. Pole offset, magnet thickness, pole embrace and stator slot dimension are input parameters for optimization. In first, a PMSM designed and then is evaluated by using FEA, in continue PSO algorithm is combined with FEA and in each iteration of PSO, FEA is used to calculate the optimization goals. The continuation of this article is as follows. Section II presents the design equations and specification of designed PMSM. In section III, proposed the optimization procedure. Finally, this paper introduces an analysis of the PMSM performance and results of optimization.

## 2. Design Process of PMSM

Design process of an electrical machine is iterative and the number of steps depends on a number of restrictions to be met simultaneously. Design process of a PMSM consist of following steps:

### A. Design primary parameters

The primary specification and main parameters of a PMSM for optimization, presented in “Table 1”.

Table 1. Preliminary design specification

Parameter [Symbol (unit)]	Stator	Rotor
<b>Initial Specification</b>		
Generator Power [P (kW)]	22	
Efficiency [ $\eta$ (%)]	94	
Power Factor [PF]	0.93	
Line Voltage [ $U_s$ (V)]	400	
Number of Poles [2p]	8	
Number of Phases [m]	3	
Frequency [f (Hz)]	100	
<b>Assumptions</b>		
Linear Current Density [A (kA/m)]	35	
Air-gap Flux Density [ $B_\delta$ (T)]	0.9	
Tooth Flux Density [ $B_{ds}$ (T)]	1.6	-
Yokes Flux Density [ $B_{ys,r}$ (T)]	1.4	1.4
Current Density [ $J_s$ (A/mm <sup>2</sup> )]	5.5	-
Number of Slots [ $Q_s$ ]	48	-
Space Factor of the Core [ $k_{fc}$ ]	0.95	0.95
Pole-Shoe Arc to Pole Pitch Ratio [ $\alpha_i=b_p/\tau_p$ ]	0.8	
No Load to Rated Load Terminal Phase Voltage Ratio [ $\varepsilon=E_m/U_{ph}$ ]	0.86	

### B. Geometric Dimension of the PMSM

The most interesting mechanical dimension are the actual length of the machine and the stator outer diameter, because these two roughly determine the machine size. To be able to construct the mechanical parts of the machine, also the detailed dimensions for the stator and rotor are

needed. In the case of the stator, the inner and outer diameters of the stator core, the height of the yoke and the teeth, the width of the teeth, the slot dimension and the number of slots need to be found. The rotor dimensions in this case are the rotor inner and outer diameter [16-18]. The geometric dimension of the studied PMSM shown in "Figure. 1".

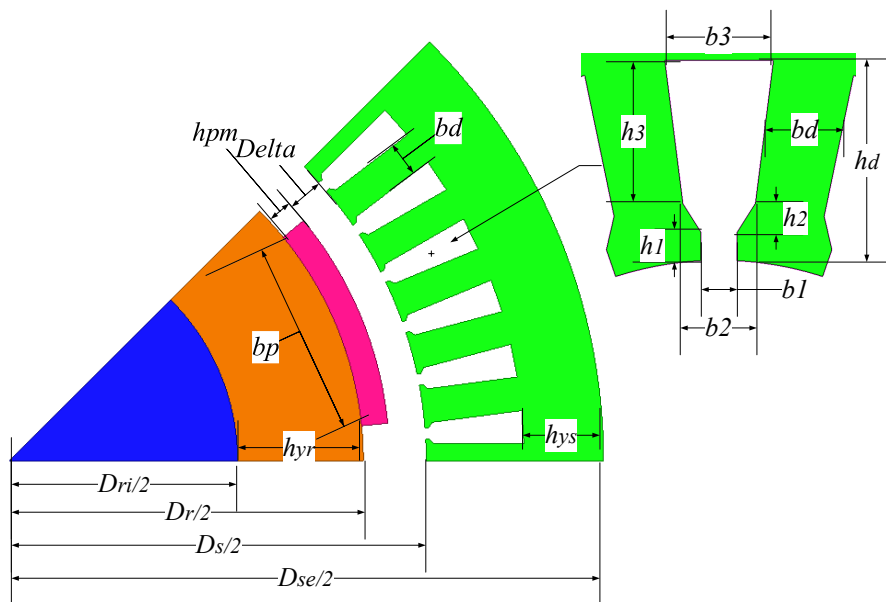


Figure 1. Topology of the studied motor

Stator inner diameter ( $D_s$ ) of motor can be calculated as

$$D_s = \sqrt[3]{\frac{P_{out} \times \varepsilon}{C \times n_s \times \chi}} \quad (1)$$

In (1),  $C$  is machine constant,  $n_s$  is speed in round per second (rps) and  $\chi$  is ratio of the effective machine length to the Stator inner diameter. This parameters are as

$$C = 0.5\pi^2 k_{ws1} AB \cos \varphi \quad (2)$$

$$n_s = \frac{f}{2p} \quad (3)$$

$$\chi = \frac{l'}{D_s} \cong \frac{\pi}{4p} \sqrt{p} \quad (4)$$

Therefore effective machine length would be  $l' = \chi D_s$ . Also, air-gap length of a PMSM ( $\delta$ ) estimated as

$$\delta = \gamma \tau_p \frac{A}{B_\delta} \quad (5)$$

Where  $\gamma$  is a coefficient and its value for different conditions presented in [17]. Pole pitch in meter and slot number, slot pitch in meter and number of slots per phase per pole are obtained by following equation respectively

$$\tau_p = \frac{\pi D}{2p} \quad (6)$$

$$y_Q = \frac{Q_s}{2p} \quad (7)$$

$$\tau_u = \frac{\pi D}{Q_s} \quad (8)$$

$$q_s = \frac{Q_s}{2pm} \quad (9)$$

Winding factor can be calculated as

$$k_{ws1} = \sin\left(\frac{y}{y_Q} \cdot \frac{\pi}{2}\right) \cdot \frac{1}{2q_s \sin\left(\frac{\pi}{6q_s}\right)} \quad (10)$$

In this machine chosen a two layer winding for winding of stator and also, in order to reduce space harmonics coil pitch/pole pitch ratios for stator is chosen as 6/8. The number of the coil turns in series in a phase winding for stator are obtained by

$$N_s = \frac{E_m}{\sqrt{2}\pi k_{ws1} \phi_{\delta,PM}} \quad (11)$$

$\Phi_{\delta,PM}$  is maximum magnetic flux in the air-gap. Number of conductors per slot becomes

$$z_{Q_s} = \frac{2m}{Q_s} N_s \quad (12)$$

### C. Slot and Tooth Dimension

In this design, semi closed slots have been considered in accordance with “Figure. 1”. Areas of the stator conductors and stator slots determined by

$$S_{cs} = \frac{I_s}{J_s} \quad (13)$$

$$S_{us} = \frac{z_{Q_s} S_{cs}}{k_{fill}} \quad (14)$$

Where  $k_{fill}$  is space factor of the stator slot and depends to voltage level. It's value in this design considered 0.5. Now, slot area is obtained through geometric relations

$$S_{us} = \frac{1}{2}(b_2 + b_3)h_3 \quad (15)$$

Where  $b_2$  and  $b_3$  are as follows

$$b_2 = \frac{\pi(D_s + 2h_1 + 2h_2)}{Q_s} - b_d \quad (16)$$

$$b_3 = \frac{\pi(D_s + 2h_1 + 2h_2 + 2h_3)}{Q_s} - b_d \quad (17)$$

Also, the teeth width are obtained from following equation

$$b_d = \frac{l' \tau_u}{k_{fe} l} \cdot \frac{B_{\delta}}{B_{ds}} + 0.1mm \quad (18)$$

0.1 is influence of punching on the crystal structure and permeability of iron. By solving (15), (16) and (17), we can obtain two unknown parameters  $h_3$  and  $b_3$ . Values of  $b_1$ ,  $h_1$  and  $h_2$  are 3, 1 and 1 mm respectively.

In this work, we have been used from semi-closed slots for stator. In case of semi-closed slots the slotting effect can be taken into account by the Carter factor.

### D. Stator and Rotor Yokes Height

Stator and rotor yokes height are calculated as

$$h_{ys,r} = \frac{\varphi_{\delta,PM}}{2k_{fe}lB_{ys,r}} \quad (19)$$

Intended iron lamination for stator and rotor core is M19-29G.

#### E. Permanent Magnet Dimension

Permanent magnet used in studied machine is NdFeB30. Specification of this magnet presented in “Table 2”. Permanent magnet length ( $l_{pm}$ ) would be equal to the effective length of the machine. Also, magnet width ( $b_p$ ) and thickness ( $h_{pm}$ ) can be calculated as

$$b_p = \alpha_i \tau_p \quad (20)$$

$$h_{pm} = \frac{B_{\delta} k_c \delta \mu_{PM}}{B_r - B_{\delta} k_c} \quad (21)$$

Where  $k_c$  is carter coefficient and can be calculated as

$$\kappa_s = \frac{b_1 / \delta}{5 + b_1 / \delta} \quad (22)$$

$$\kappa_c = \frac{\tau_u}{\tau_u - \kappa_s b_1} \quad (23)$$

Table 2. Specification of the NdFeB30

Parameter	Symbol (Unit)	Value
Residual Flux Density	$B_r$ (T)	1.1
Coercive Force	$H_c$ (kA/m)	838
Relative Permeability	$\mu_{PM}$	1.0446

#### F. Magnetic Circuit Calculation

In this section magnetic flux and air-gap flux density are calculated. For this purpose, a reluctance network model of the PMSM is employed. In “Figure. 2” a reluctance network for a surface mounted PMSM is proposed. Air-gap flux can be derived from the equivalent reluctance circuit

$$\varphi_{\delta,PM} = \frac{\Theta_{PM}}{R_{PM} + R_{\delta} + R_{Fe} + \frac{R_{PM}}{R_{\delta 2}} (R_{\delta} + R_{Fe})} \quad (24)$$

Where  $\Theta_{PM} = h_{pm} \times H_c$ . The reluctance of the air-gap between the permanent magnets and stator

$$R_{\delta} = \frac{\delta_e}{\mu_o \tau_p l'} \quad (25)$$

The reluctance of the air-gap between two magnets is

$$R_{\delta 2} = \frac{h_{pm}}{\mu_o (\tau_p - b_p) l'} \quad (26)$$

Reluctance of the permanent magnets is

$$R_{PM} = \frac{h_{pm}}{\mu_o \mu_{PM} b_p l'} + \frac{l_i}{\mu_o b_p l'} \quad (27)$$

Where  $l_i$  is the thickness of the insulation layer between the rotor and the magnets. The iron reluctance is

$$R_{Fe} = \frac{h_{ds}}{\mu_o \mu_{Fe} b_d l'} + \frac{w_{ys}}{\mu_o \mu_{Fe} h_{ys} l'} \quad (28)$$

Where  $h_{ds}$  is tooth height,  $\mu_{Fe}$  is permeability of iron,  $w_{ys}$  is the yoke width and can be calculated as

$$w_{ys} = \frac{\pi(D_{se} + D_s + 2h_{ds})}{4p} \quad (29)$$

Finally, the air-gap flux density is derived from the air-gap flux and width of permanent magnets as well as from the effective length

$$B_{\delta} = \frac{\varphi_{\delta,PM}}{b_p l'} \quad (30)$$

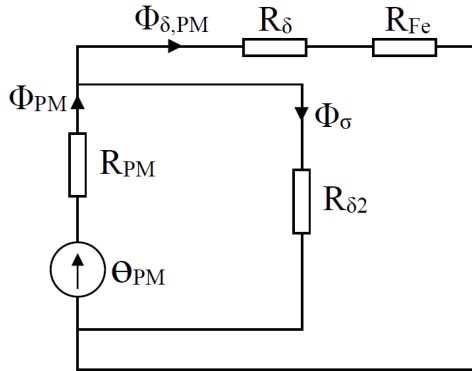


Figure 2. Equivalent reluctance circuit for a PMSM with surface mounted magnets

The studied motor in this paper is a Surface Mounted Permanent Magnet Synchronous Motor. In Surface Mounted PMSM, because of the rectangular air-gap flux density the flux densities in the stator teeth are constants above the permanent magnets and become zero elsewhere. The rectangular air-gap flux density of the SPMSM means that the calculation of the saturation form factor is not any more required here.

### 3. PSO Algorithm

In this paper, PSO algorithm is used for optimization of studied PMSM. PSO is a population based stochastic optimization technique, inspired by social behavior of bird flocking or fish schooling or ant colonies. This algorithm emulates the interaction between members to share information. PSO has been applied to numerous areas in optimization and in combination with other existing algorithm. This method performs the search of the optimal solution through agents, referred to as particles, whose trajectories are adjusted by a stochastic and a deterministic component. Each particle is influenced by its best achieved position and the group best position, but trends to move randomly. One of the advantage of PSO optimization over other derivate free methods is the reduced number of parameters to tune and constraints acceptance [20].

In “Figure. 3” is shown flowchart of presented design and optimization method. In the first stage initial parameters are determined and then geometric dimensions are calculated. In stage 3, magnet width and thickness are estimated and in stage 4, air-gap flux and flux density are calculated using (11). In stage 5, slot and tooth dimension are determined. In stage 6, new values for the air-gap flux and flux density are defined by calculating the iron reluctance. Steps 4-7 are repeated until the air-gap flux density does not change more than determined error. Then in the 8-9, induced electrical voltage is calculated in full load ( $E_s$ ), and steps 2-9 repeat until the voltage  $E_s$  in comparison to the no load induced voltage ( $E_m$ ) does not change more than determined error. The rest of the machine properties are calculated during step 10. After determining all parameters of machine, results validation are checked by using FEA tools. In step 12-13, goals optimized by using PSO algorithm. Steps 11-13 repeat until getting the best results.

#### 4. Optimization Formulation

First considered cost function in this paper is cogging torque. Based on [21], magnet dimension and slot dimension are solutions for reduction of cogging torque. Therefore, if this two dimensions of motor optimize, cogging torque will reduction. In this paper we have used a combination of this two method. In other words, both magnet and stator slot dimension are supposed for reduction of cogging torque. Optimized dimension is found by an iterative process and PSO algorithm.

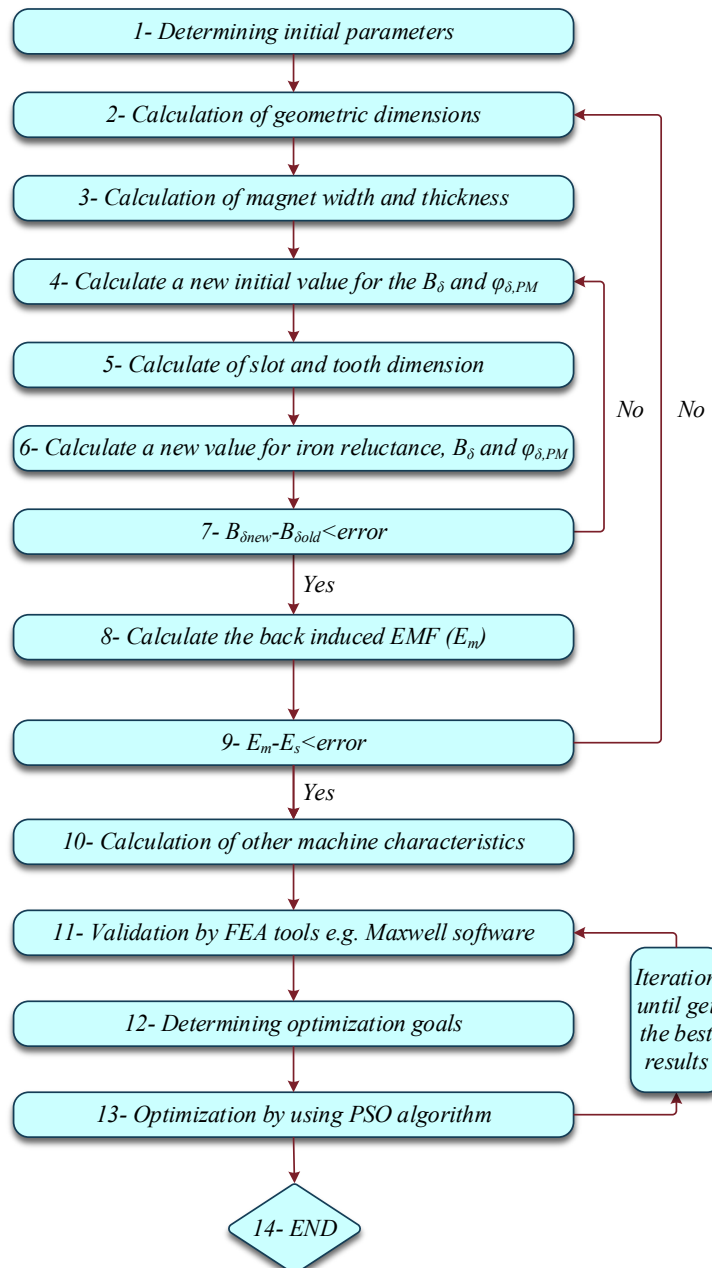


Figure 3. Flowchart of the design and optimization process

Other cost function in this paper is efficiency. If we can reduce motor losses, efficiency will improve. Two motor losses are copper loss and core loss of stator and resistance of stator is effective on them. Stator and rotor resistance also depends on Slot dimensions. This problem affects the copper loss and core loss i.e. the variation in slot dimensions causes change in copper loss and core loss and finally the variation in mentioned losses is effective in efficiency. Stator resistance can be calculated as [19]

$$R = \left[ (k_{Ru} - 1) \frac{2l'}{l_{av}} + 1 \right] R_b \quad (31)$$

Where  $R_b$  is the resistance without consideration skin effect,  $l_{av}$  is the average length of the coil turn and  $k_{Ru}$  denotes the average resistance factor that its value is calculated as

$$k_{Ru} = \xi \frac{\sinh 2\xi + \sin 2\xi}{\cosh 2\xi - \cos 2\xi} + \frac{z_t^2 - 1}{3} \cdot 2\xi \frac{\sinh \xi - \sin \xi}{\cosh \xi + \cos \xi} \quad (32)$$

$$\xi = h_3 \sqrt{\frac{1}{2} \omega \mu_c \sigma_c \frac{b'_3}{b_3}} \quad (33)$$

Where  $z_t$  is the number of conductor layers,  $\omega$  is the angular frequency,  $\sigma_c$  is the specific conductivity of the copper or aluminum used as conductor.  $b'_3$ ,  $b_3$  and  $h_3$  are also shown in Figure. 4.

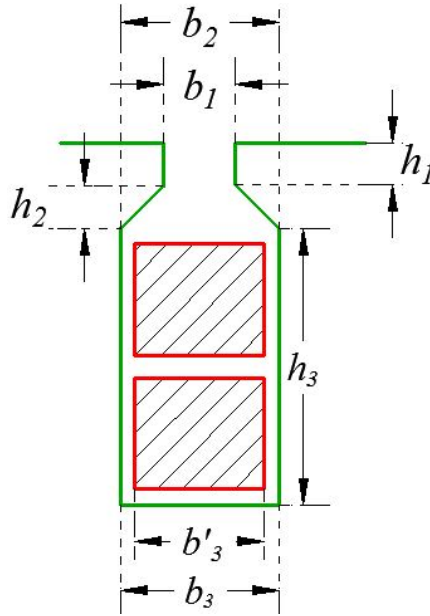


Figure 4. Dimensions required for calculate of stator and rotor resistance

## 5. Design and Optimization Results

In this section, the results of the designed PMSM are presented. Air-gap flux density final value reaches to 0.85 T. In order to verify the analytical design process with Matlab software, considered PMSM were simulated in Maxwell software which is a FEA tool. A comparison between analytical and FEA design results are done and presented in “Table 3”. Magnetic flux density and flux lines distribution at 2 second and in one eighth cross section of PMSM shown in “Figure. 5”. As can be seen from this Figure, the created rotor and stator flux density in different parts of machine are lower than the magnetic saturation value of the lamination material (2.5 T). Also, meshing diagram of PMSM finite element model shown in “Figure. 6”.

Table 3. Comparison between analytical and FEA design

Symbol (unit)	Analytical Design		FEA	
	Stator	Rotor	Stator	Rotor
$B_{\delta}$ (T)	0.85		0.831	
$B_{ds}$ (T)	1.6	-	1.56	-
$B_{ys,r}$ (T)	1.4	1.4	1.39	1.389
$J_s$ (A/mm <sup>2</sup> )	5.5	-	5.509	-
A (kA/m)	35		35.8	
Efficiency (%)	94.4		95.2	
Cogging torque	6.32		6.87	

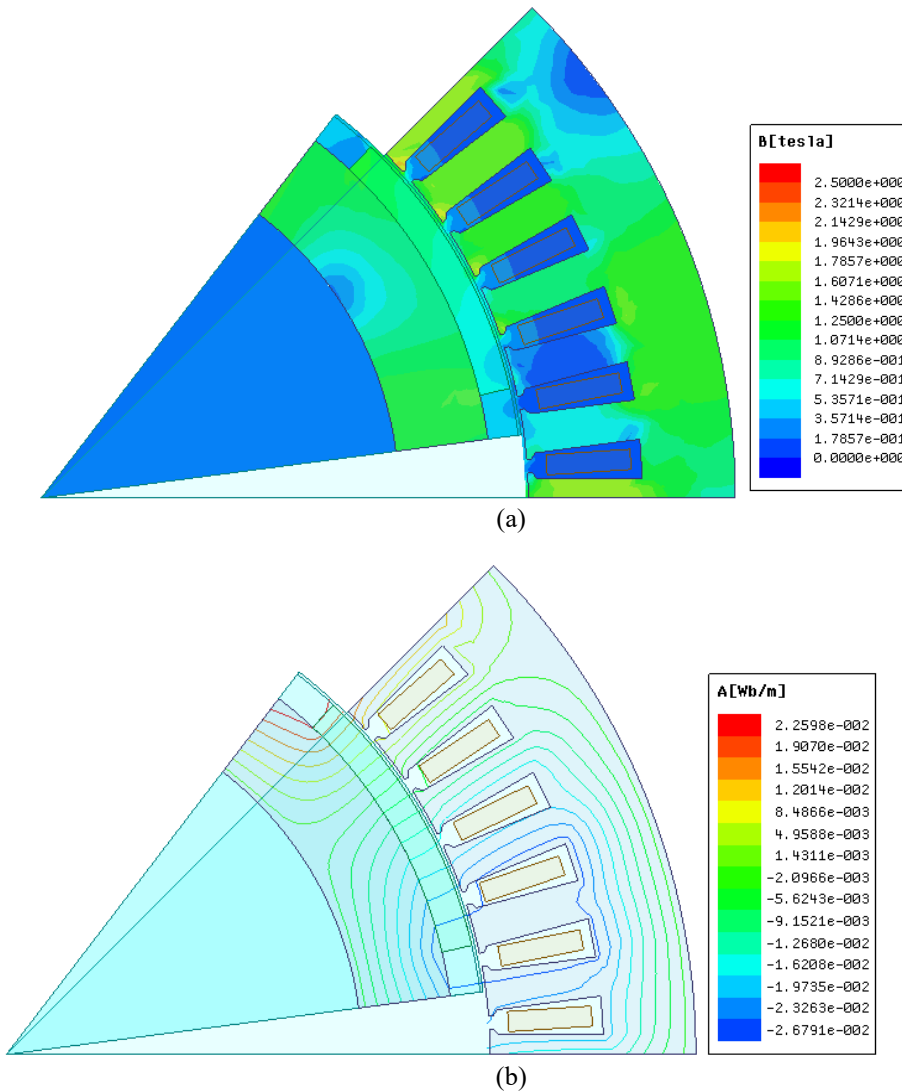


Figure 5. (a) Magnetic flux density and (b) Magnetic flux lines of the designed PMSM

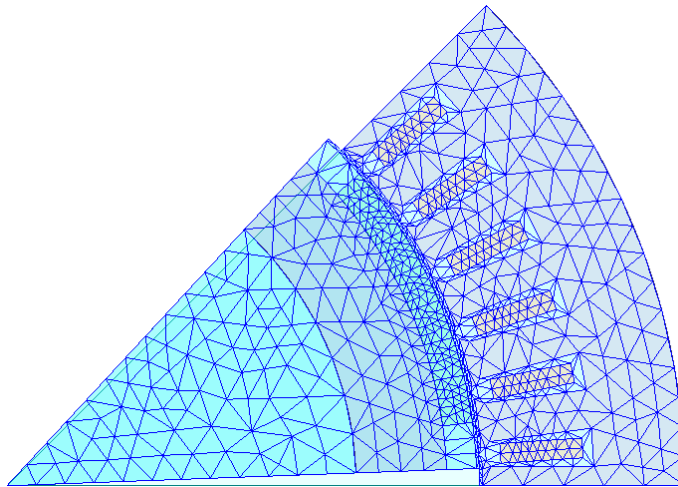


Figure 6. Meshing diagram of the designed PMSM

Sensitivity analysis has been done and results have been shown in Figure. 7. Pole offset and  $b_{s2}$  selected as sensitivity variable parameters and their effect studied on Efficiency and cogging torque. Effect of two mentioned parameters on efficiency and cogging torque has been shown in Figure. 7 (a) and Figure. 7 (b) respectively. It can be seen from Figure. 7 (a) that lower value for pole offset causes higher efficiency. We can also see from Figure. 7 (b) that lower value for cogging torque is gained by higher value for pole offset.

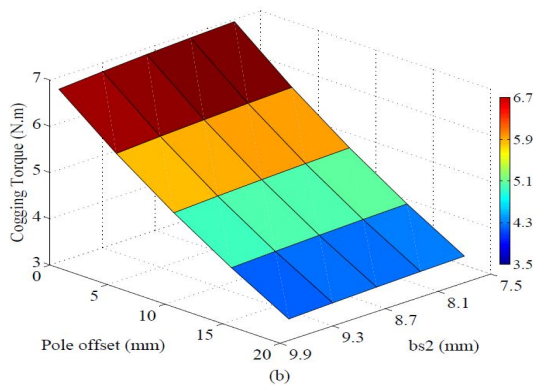
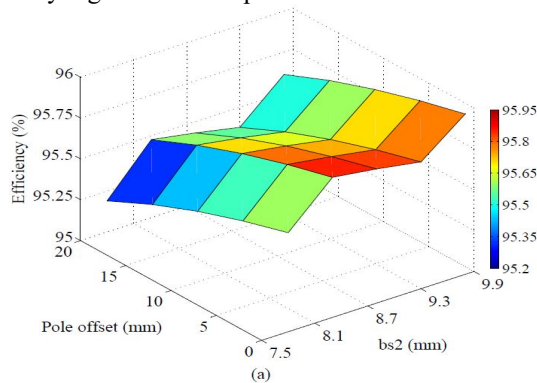


Figure 7. Effect of pole offset and stator slot dimension variation on (a) Efficiency  
(b) Cogging torque

Table 4. Optimization parameters boundaries

Parameter (mm)	Lower limit	Upper limit
$b_1$	2.7	3.3
$b_2$	5	6.5
$b_3$	7.8	9.8
$h_3$	18	28
Pole embrace	0.6	0.9
Pole offset	0	20
$h_{pm}$	5.5	7.5

Table 5. Optimization results

Parameter (unit)	Reference model	Low Cogging torque	High efficiency
$b_1$ (mm)	3	3	3
$b_2$ (mm)	5.6936	6.3888	5.6213
$b_3$ (mm)	8.7961	9.0840	8.0085
$h_3$ (mm)	23.7012	22.106	24.2176
Pole embrace (mm)	0.7479	0.84	0.858
Pole offset (mm)	0	18.6283	0
$h_{pm}$ (mm)	6.9	6.6455	6.924
Efficiency (%)	95.2	94.9	96.16
Cogging torque (Nm)	6.87	0.347	5.158
Output torque (Nm)	140.098	140.105	140.115
Output power (kW)	22.0066	22.0076	22.0092
$J_s$ (A/mm <sup>2</sup> )	5.509	5.68	5
$A$ (kA/m)	35.8	36.2	34.1
$B_\delta$ (T)	0.831	0.82	0.89
$B_{ds}$ (T)	1.56	1.62	1.52
$B_{ys}$ (T)	1.39	1.38	1.58
$B_{yr}$ (T)	1.389	1.42	1.54

Reduction of cogging torque and increase of efficiency are optimization goals and magnet pole embrace, pole offset and magnet thickness are optimization input parameters. Boundaries of input parameters presented in “Table 4”. Optimal parameters for each cost function obtain by PSO algorithm and then in each step this parameters insert in Ansys Maxwell model. This process is repeated until the best results for each cost function are obtained. Optimization results i.e. reduce of cogging torque and increase of efficiency are presented in “Table 5”. As can be seen from “Table 5” input and output parameters have been compared between reference model, low cogging torque and high efficiency. While optimization goal is “low cogging torque”, cogging torque value reaches to 0.347 Nm, however, this value for reference model is 6.87 Nm. Also, while optimization goal is “high efficiency”, efficiency value reaches to 96.16%, however, this value for reference model is 94.92%. Other important parameters e.g. current density, linear current density, flux density in yokes, teeth and air-gap are in allowed range.

Moving torque of designed PMSM for reference model, cogging torque reduction and high efficiency goals are shown in “Figure. 8”. As can be seen from this Figure, cogging torque in second state is lower than two other state. Also, the total losses are shown in “Figure. 9”. In this state, the total losses in third state are lower than two other state.

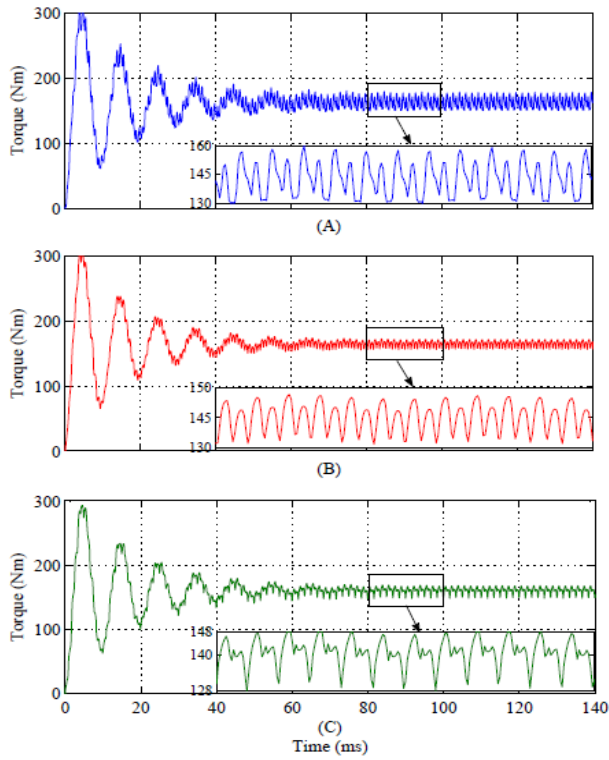


Figure 8. Moving Torque in (A) Reference model (B) Low cogging torque and (C) High efficiency

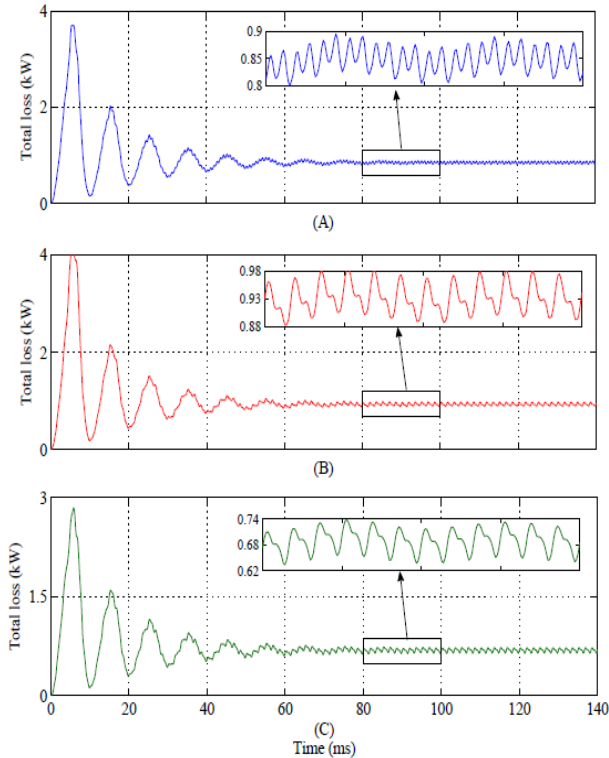


Figure 9. Total losses in (A) Reference model (B) Low cogging torque and (C) High efficiency

## 6. Conclusion

In this paper a new method for optimization of a PMSM is presented. Optimization goals are low cogging torque and increase of efficiency. Pole embrace, pole offset, magnet thickness and stator slot dimension are considered as input parameters for optimization. PSO algorithm which is a population based stochastic optimization technique used for optimization of goals. In first by using analytical method, motor is designed and then for validation of designed motor a FEA tool e.g. Maxwell or Flux software is used. In continue, PSO in combination with FEA used to increase of efficiency and reduce of cogging torque in a PMSM. In each iteration of PSO, FEA is used to calculate the optimization goals. Results of design and optimization show effectiveness and capability of proposed method.

## 7. References

- [1]. K. Ismail, T. D. Rachmildha, E. Rijanto, and Y. Haroen, "A Hybrid Cross Coupling – Master Slave Technique for Speed Synchronization of Multi PMSMs System Using PID Controller and On-Line Master Selector," *International Journal on Electrical Engineering and Informatics*, Vol. 11, No. 1, pp. 183–194, Mar. 2019.
- [2]. S. K. Injeti, and M. Divyavathi, "Optimal Gain Scheduling of PID Controller for the Speed Control of PMSM Drive Using Bio-Inspired Optimization Algorithms," *International Journal on Electrical Engineering and Informatics*, Vol. 11, No. 2, pp. 308–325, Jun. 2019.
- [3]. M. N. Nashed, A. M. Sharaf, and M. N. Eskander, "A Fuzzy Logic Fault Ride-Through Scheme for Electric Vehicles Using PMSM-AC Drives," *International Journal on Electrical Engineering and Informatics*, Vol. 12, No. 1, pp. 129–140, Mar. 2020.
- [4]. A. Izanlo, S. Asghar Gholamian, and M. V. Kazemi, "Comparative Study Between Two Sensorless Methods for Direct Power Control of Doubly fed Induction Generator," *Rev. Roum. Sci. Tech. – Electrotechn. et Energ.*, Vol. 62, No. 4, pp. 358-364, Dec. 2017.
- [5]. Guo, Z. Wu, H. Qian, and Z. Sun, "Robust Design for the 9-Slot 8-Pole Surface Mounted Permanent Magnet Synchronous Motor by Analytical Method Based Multi Objective Particle Swarm Optimization," *IET Electric Power Applicat.*, Vol. 10, No. 2, pp. 117–124, Feb. 2016.
- [6]. Hong, T. Wei, and X. Ding, "Multi-Objective Optimal Design Synchronous Motor for High Efficiency and High Dynamic Performance," *IEEE Access.*, Vol. 6, pp. 23568–23581, April 2018.
- [7]. Y. Sui, P. Zheng, P. Tang, F. Wu, and P. Wang, "A Five-Phase 20-Slot/18-Pole PMSM for Electric Vehicles," *International Journal for Computation and Mathematics in Electrical and Electronic Engineering*, Vol. 35, No. 2 pp. 439–455, April 2018.
- [8]. Bakhtiarzadeh, A. Polat, and L. Ergene, "Design and Analysis of a Permanent Magnet Synchronous Motor for Elevator Applications," *In OPTIM & ACEMP conference*, March 2016.
- [9]. M. Soleimani, and S. Gholamian, "Optimum Design of a Three-Phase Permanent Magnet Synchronous Motor for Industrial Applications," *International Journal of Applied Operational Research*, Vol. 3, No. 1, pp. 67–85, Dec. 2013.
- [10]. A. Nikbakhsh, H. Izadfar, and Y. Alinejad, "Design and Optimization of Permanent Magnet Synchronous Generator for Use in Hydrodynamic Renewable Energy by Applying ACO and FEA," *IJUM Engineering Journal*, Vol. 18, No. 2, pp. 158-176, Dec. 2017.
- [11]. Z. Guo, L. Chang, and Y. Xuo, "Cogging Torque of Permanent Magnet Electric Machines: An Overview," in *CCECE*, pp. 1172-1177, Ma 2009.
- [12]. Y. ÖZOĞLU, "New Magnet Shape for Reduction torque ripple in an Outer Rotor Permanent Magnet Machine," *Turkish Journal of Electrical Engineering & Computer Sciences*, Vol. 25, No. 5, pp. 4381–4397, Oct. 2017.
- [13]. C. Lim, J. K. Woo, G. H. Kang, J. P. Hong, and G. T. Kim, "Detent Force Minimization Techniques in Permanent Magnet Linear Synchronous Motors," *IEEE Trans. Magn.*, Vol. 38, No. 2, pp. 1157-1160, March 2002.

- [14]. S. M. Hwang *et. al.*, “Various Design Techniques to Reduce Cogging Torque by Controlling Energy Variations in Permanent Magnet Motors,” *IEEE Trans. Magn.*, Vol. 37, No. 4, pp. 2806-2809, July 2001.
- [15]. Q. He, and X. Bao, “Reducing Cogging Torque in Permanent Magnet Synchronous Motors by Auxiliary Teeth Method,” in *ICIEA Conference*, Oct. 2016.
- [16]. Sato, J. S. Shin, T. Koseki, and Y. Aoyama, “Basic Experiments for High Torque, Low Speed Permanent Magnet Synchronous Motor and a Technique for Reducing Cogging Torque,” in *ICEM*, Sept. 2010.
- [17]. Manninen, “Evaluation of the Affects of Design Choices on Surface Mounted Permanent Magnet Machines Using an Analytical Dimensioning Tool,” Master Thesis, Aalto University, Espoo, 2012.
- [18]. J. Pyrhonen, T. Jokinen, V. Hrabovcova, “Design of Rotating Electrical Machines,” Wiley, Second Edition, 2014.
- [19]. Boldea, S. Nasar, “The Induction Machines Design Handbook,” Boca Raton, FL, USA: CRC Press, 2010.
- [20]. S. Chacko, Ch. N. Bhende, Sh. Jain, and R. K. Nema, “Rotor Resistance Estimation of Vector Controlled Induction Motor Drive Using GA/PSO tuned Fuzzy Controller,” *International Journal on Electrical Engineering and Informatics*, Vol. 8, No. 1, pp. 218-236, Mar. 2016.
- [21]. R. Krishnan, “Permanent Magnet Synchronous and Brushless DC Motor Drives,” Boca Raton, USA: CRC Press, 2010.



**Ali Izanlo** was born in Shirvan, Iran, in 1990. He received his BSc degree in electrical engineering from Birjand University, Birjand, Iran in 2009. He received his MSc degree from Noshivani University of Technology in Mazandaran, Iran. His current research interests include variable and adjustable speed power generation with permanent magnet and doubly fed induction generators, automotive power electronics and drives, and current measurement systems for power electronics.



**S. Asghar Gholamian** was born in Babolsar, Iran, in 1976. He received his BSc degree in electrical engineering from K.N. Toosi University of Technology, Tehran, Iran in 1999 and his MSc degree in electric power engineering from the University of Mazandaran, Babol, Iran in 2001. He also received his PhD in electrical engineering from K.N. Toosi University of Technology, Tehran, Iran in 2008. He is currently Assistant Professor in the Department of Electrical Engineering at the Babol University of Technology, Iran. His research interests include power electronic and design, simulation,

modeling, and control of electrical machines.



**S. Ehsan Abdollahi** was born in Babol, Iran, in 1980. He received his BSc degree in electrical engineering from Amirkabir University, Tehran, Iran in 2002 and he received his MSc degree in electrical engineering from Iran University of Science & Technology, Tehran, Iran in 2005. He also received his PhD in electrical engineering from University of Tehran, Tehran, Iran. His research interests include electric machinery, motor control, power electronics, and renewable energy conversion.